

# Aging and Reliability of Quantum Networks

Lisa T. Weinbrenner,<sup>1</sup> Lina Vandré,<sup>1,2</sup> Tim Coopmans,<sup>3</sup> and Otfried Gühne<sup>1</sup>

<sup>1</sup>*Naturwissenschaftlich-Technische Fakultät, Universität Siegen, Walter-Flex-Straße 3, 57068 Siegen, Germany*

<sup>2</sup>*State Key Laboratory for Mesoscopic Physics, School of Physics and Frontiers*

*Science Center for Nano-Optoelectronics, Peking University, Beijing 100871, China*

<sup>3</sup>*Leiden Institute of Advanced Computer Science, Leiden University, Leiden, The Netherlands*

(Dated: June 1, 2023)

Quantum information science may lead to technological breakthroughs in computing, cryptography and sensing. For the implementation of these tasks, however, complex devices with many components are needed and the quantum advantage may easily be spoiled by failure of few parts only. A paradigmatic example are quantum networks. There, not only noise sources like photon absorption or imperfect quantum memories lead to long waiting times and low fidelity, but also hardware components may break, leading to a dysfunctionality of the entire network. For the successful long-term deployment of quantum networks in the future, it is important to take such deterioration effects into consideration during the design phase. Using methods from reliability theory and the theory of aging we develop an analytical approach for characterizing the functionality of networks under aging and repair mechanisms, also for non-trivial topologies. Combined with numerical simulations, our results allow to optimize long-distance entanglement distribution under aging effects.

*Introduction.*— Modern experimental science is based on complex technical devices for measuring and manipulating physical systems. Examples are the Large Hadron Collider for testing the limits of the standard model and the observatory LIGO for detecting gravitational waves. All these experimental setups consist of many different parts, which must be functional for the whole device to be operational. In quantum technologies, typical setups include quantum computers or quantum networks which consist of many smaller quantum systems. These constituents are not only prone to decoherence and noise, but they may also fail completely. For overcoming this, redundancy and quantum error correction can be used and there is a trade-off between the required redundancy and the quality of the elementary devices. This trade-off is also relevant for comparing different quantum computing platforms, such as solid-state systems with many qubits and relatively short coherence times with ion traps, which have fewer but long-lived qubits [1, 2]. For the long-term success, developing different approaches towards quantum technologies is important, but an advanced theory for analyzing the pros and cons of different implementation strategies is needed.

Besides quantum computers, quantum networks are a central paradigm of quantum technologies [3, 4]. The aim of these networks is to enable global quantum communication, but they are also useful for distributed sensing [5–7], clock synchronisation [8] and blind quantum computation [9]. Consequently, there are many theoretical proposals for robust and efficient networks, using techniques like quantum repeaters [10–13], multiplexing [14–17] and advanced quantum state encodings [18–20]. In the last years, different building blocks of quantum networks were experimentally demonstrated, such as quantum teleportation between non-neighboring nodes [21],

satellite to ground communication [22] and multiplexing [23, 24]. All these implementations are, apart from the ubiquitous noise and photon loss, subject to deteriorating effects: devices may be defect from the beginning or get destroyed during the experiment. In practice, devices may also fail only temporarily, due to, for example, overheating. While noise and loss in networks have been discussed in detail and may be overcome by entanglement purification, error correction and other heralded procedures [20], the effects of aging, breaking and repairing of hardware components are rarely studied. The present literature closest to this topic focuses on the waiting times and quantum-state quality for the functionality of a chain [14, 25–34], where temporary hardware failure and recovery are absent, or global success probabilities for networks [35, 36], where the topological structure of a specific network is often not taken into account. For a full characterization of aging effects and reliability, three main difficulties arise: First, the devices are highly dependent on each other due to feedback loops. Second, the topologies of networks are inherently more complicated than simple repeater chains. Third, the temporary failures of single devices may lead to non-Markovian effects.

The goal of this paper is twofold: First, we show how ideas and concepts from reliability theory [37–39], known from sociology and the theory of aging, can be applied to the analysis of quantum networks. Second, we develop an analytical theory for discussing temporary failure and repairing in quantum networks. In contrast to classical networks, where adding redundant hardware is cheap, current quantum hardware is fragile so that it is essential to have complete understanding of the network behaviour to find the optimal protocols for it. Our approach differs from network percolation theory [40, 41] by focusing on the temporal failure and recovery and is

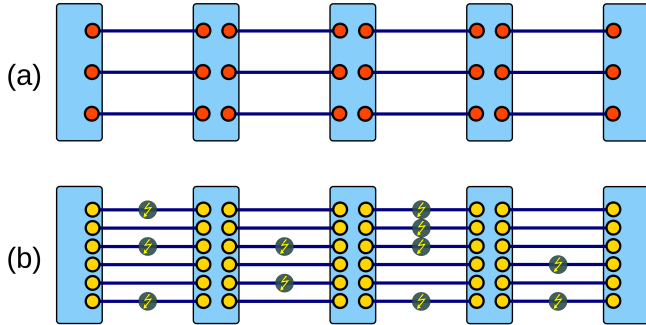


FIG. 1. (a) Schematic view of a multiplexed repeater chain, with  $M + 1 = 5$  nodes and  $M = 4$  edges, each edge having a multiplicity of  $N = 3$ . (b) Alternative approach for the implementation of a similar repeater chain, where initially  $N = 6$  physical connections have been established within the edges, but some of them are not functioning from the beginning. In this example, on average three physical connections are working. In the depicted example, there are two connections between the end nodes (as one edge contains only two working connections), so the flux of the entire chain is two. Interestingly, both approaches, although being initially on average the same, can exhibit fundamentally different behaviour on the long time scale.

in line with recent work on fabrication defects in planar quantum computers [42]. The presented methods lead to various results. First, depending on a given figure of merit for the entire network, we can specify which type and quantity of the redundant devices like quantum memories and entanglement sources are needed. Second, we can characterize the non-Markovian temporal behavior of a quantum network depending on the failure and repairing of each single device. Third, our results lead to bounds on the parameters of quantum protocols performed on these networks. As a main example we use the suggested configuration for a real quantum network in the Netherlands [43], but our results are easily extendable to more complex topologies.

*Quantum networks.*— It is the general aim of a quantum network to generate entanglement in two distinct, far apart stations. A direct exchange of entangled particles transmitted through glass fibre, however, has an exponentially with the distance increasing loss probability. Therefore, one can use the concept of a quantum repeater [10–12], where several intermediate repeater stations are built between the end stations (see Fig. 1). Entanglement is first created and stored between adjacent repeater stations and then converted to long-range entanglement via Bell measurements within the stations. This setup allows to overcome the exponential loss scaling. More generally, a quantum network may consist of many nodes which are connected by edges in various ways, leading to a complicated topology.

In order to explain our main ideas, we first focus on a

simple network, the so-called repeater chain, consisting of  $M + 1$  nodes connected with  $M$  edges in a linear configuration, see also Fig. 1. We allow multiplexing within the edges, meaning that each edge consists of  $N$  physical connections. Each connection can be seen as a physical system, where entanglement may be established, e.g., a spatial or spectral mode of a fiber for photons. The concept of multiplexing was introduced to allow for higher entanglement generation rates [14].

Our main aim is to characterize at which times the network is functional if some devices or connections break down permanently or become dysfunctional for a certain time, e.g., due to ice formation on a chip in a cryostat, overheating, or mechanical failures. So, instead of describing the entanglement generation process and its time scales (as it has been done in Refs. [14, 35, 44], for example), we want to describe the functionality of the entire network depending on the functioning of each single device.

*The theory of aging.*— Biological and technical systems typically consist of many parts, with a complex structure of functional dependencies. This raises the problem how long the entire system is functional, if some of the parts fail. The description of the reliability of such a complex system is the main goal of reliability theory [37, 39]. The two main quantities are the reliability function

$$S(t) = \mathbb{P}(T > t), \quad (1)$$

which denotes the probability for a failure to occur at the failure time  $T$  *after* time  $t$ , so it describes the probability for the system to work at least until time  $t$ . This directly allows to compute the mean time to failure via  $\langle T \rangle = \int dt S(t)$ . The failure rate

$$\mu(t) = -\frac{\partial_t S}{S} = -\partial_t \ln S(t) \quad (2)$$

describes the probability of a failure in the next time interval given the survival of the system until time  $t$ . Characteristic for the phenomenon of aging is the fact that the failure rate increases with time.

A relevant observation is that biological systems (e.g., when analyzing the death rate of humans) show a qualitatively different behaviour of the failure rate than technical devices. Typically, the failure rate of biological systems grows exponentially according to the Gompertz-Makeham law  $\mu(t) = A + Be^{\lambda t}$ , consisting of a age-independent Makeham term  $A$  and an exponentially growing Gompertz term  $Be^{\lambda t}$  [45, 46]. On the other hand, the failure of technical devices typically follows the Weibull power law [47]  $\mu(t) = at^b$ .

An intriguing connection to network theory arises from the observation that L. Gavrillov and N. Gavrillova suggested to explain the different failure rates using two different notions of redundancy, see Fig. 1. In technical systems (e.g., an aircraft), one has for each sub-component

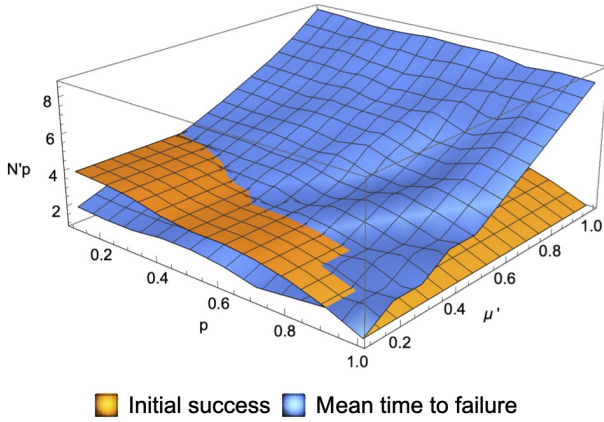


FIG. 2. Minimal multiplicity  $N'p$  required in a repeater chain with potentially initially broken devices [see Fig. 1(b)] to reach the desired functionality in terms of life time and initial success probability as a standard multiplexed chain [see Fig. 1(a)]. See text for details of the models.

(e.g., the measurement devices of the air speed) a fixed degree of redundancy, and every single part can be assumed to work in the beginning due to supervision and testing. Contrary to that, in biological systems the sub-components (e.g., the organs) have a varying degree of redundancy, since some of their cells may not work right from the beginning. Under certain assumptions it was argued in Refs. [38, 48] (but see Ref. [49] for a criticism) that the first type of redundancy leads to the Weibull law and the second type leads to the Gompertz-Makeham law.

*Aging theory for chains and networks.*— The methods from Ref. [38] can directly be extended to study the repeater chain. As implementation (a), corresponding to Fig. 1(a), we consider  $M$  edges with multiplicity  $N$ , working perfectly in the beginning, but affected by some failure rate  $\mu$ . As implementation (b), corresponding to Fig. 1(b), we consider the  $M$  edges connected with a higher multiplicity  $N' > N$ , where, however, with a certain probability  $1 - p$  each link is not working in the beginning. In practice, this may be caused by a lower quality of the devices, which are still favourable due to a lower price. In this case, the devices are affected by some failure rate  $\mu'$ . For these two implementations, we are interested in the total number of parallel connections between the end nodes; this so-called flux corresponds to the minimum of the working connections taken over all edges. Extending the methods from Ref. [38], any of these quantities can be determined fully analytically, details are given in Appendix A.

Naively, one may expect that the two implementations behave similarly, if  $N'p = N$  and  $\mu' = \mu$ , that is, the number of initially working connections in the second implementation equals *on average* the number in the first implementation. This is, however, not the case. As a

concrete example, we consider implementation (a) with  $M = 6$ ,  $N = 3$  and  $\mu = 1/2$  and implementation (b) with  $M = 6$ , varying  $p$  and varying  $\mu'$ . Then, we ask how large  $N'$  in implementation (b) needs to be such that implementation (b) has the same mean time to failure  $\langle T \rangle$  as implementation (a). This is depicted as blue surface in Fig. 2 and one finds that  $N'p$  is typically significantly larger than  $N$ , even for  $\mu' = \mu = 1/2$ .

Furthermore, in implementation (b) it is not guaranteed at all that the chain works from the beginning. So we ask (for the same parameters) how large  $N'p$  needs to be to guarantee that implementation (b) has in the beginning a working probability of at least  $p_{\text{thres}} = 0.9$  (orange surface in Fig. 2). Clearly, the lower the probability that a single connection is functioning, the higher multiplicity is needed for an initially working chain. Interestingly, for much lower failure rates  $\mu' < \mu$  this is also the determining factor for  $N'$ , if both conditions shall be satisfied. Hence we arrive at two different effects, relevant in different parameter regimes, that can be useful in determining which devices to consider when building a new network. Cheaper and imperfect devices with the same failure rate may seem tempting if the price of  $N' = N/p$  devices compared to the price of  $N$  "perfect" devices is lower. However, as derived above, one actually needs a much higher number of cheaper devices than one would naively think.

While the repeater chain may be considered as a simple toy model, future quantum networks will have complex topologies [43]. Similarly, the components of other quantum technological devices are likely to exhibit more complicated functional dependencies than the ones underlying the repeater chain. In order to demonstrate that our methods are capable of dealing with these, we consider a network as in Fig. 3 (b), which can be seen as a structural approximation of an optimized network under realistic conditions [43]. In Appendix B we derive a formalism to deal with this type of topologies using the method of indicator functions instead of probabilities. In Appendix C we present a discussion of aging effects under device failure in the topology of Fig. 3 in some detail.

*Repairing components in networks.*— Here, we consider multiplexed networks or repeater chains, where the physical connections may break down according to the models discussed above, but broken connections can be repaired. We assume that the repairing process takes several time steps.

Several questions can be asked in this situation. The first one concerns the probability that, at a given point in time, the network is functional. This is equivalent to asking for the average up-time. Second, one can ask for the probability that the entire network is broken for several consecutive time steps. Formally, this is related to the calculation of waiting times for entanglement generation in networks with finite memory [14, 26] and is challenging due to the complicated temporal dependencies of

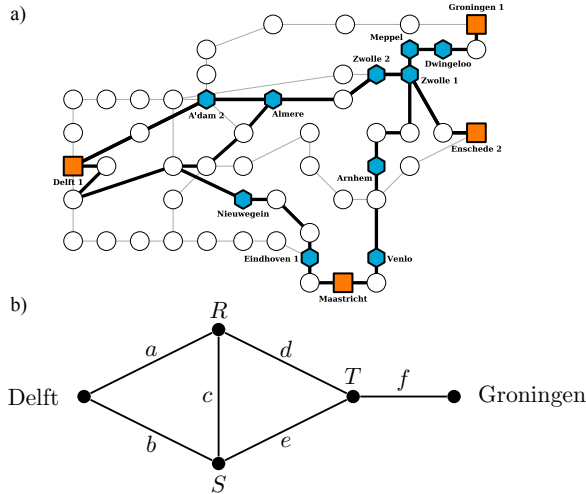


FIG. 3. (a) Optimized network topology for a network relying on the Dutch telecom infrastructure (figure taken from Ref. [43]). (b) Structural approximation of this network for a connection from Delft to Groningen. This network consists of five nodes and six connections.

the model. In the following, however, we will develop a method to tackle this.

We use for our calculations the following model: Each connection can break in a single time step with constant probability  $p_{\downarrow}$ , so the breaking of the connection is geometrically distributed. If the connection breaks, it remains non-functional for exactly  $\tau$  time steps, where  $\tau$  is a constant set in advance. After this, it is functional with probability  $(1 - p_{\downarrow})$ , but with probability  $p_{\downarrow}$  it breaks directly again, leaving it broken for at least  $2\tau$  consecutive time steps.

Since the expectation value of a geometric distribution is given by  $1/p_{\downarrow}$ , the connection is on average functional for  $1/p_{\downarrow} - 1$  time steps before breaking. The connection is thus broken on  $\tau$  out of on average  $1/p_{\downarrow} - 1 + \tau$  time steps, so the average down-time of a single connection is given by  $\tau/(1/p_{\downarrow} - 1 + \tau)$ . For a repeater chain with  $M$  edges of multiplicity  $N$  this leads to an average up-time of

$$u = \left[ 1 - \left( \frac{\tau}{\frac{1}{p_{\downarrow}} - 1 + \tau} \right)^N \right]^M. \quad (3)$$

By using more subtle counting arguments we can also calculate the probability that a chain or network displays a certain behavior in  $t$  consecutive, but arbitrarily chosen time steps. For the exact calculations we refer to Appendix D. These results can be used to characterize the "non-Markovianity" of the system. If the system behaves in a Markovian way, one expects the probability for a certain behavior in  $t$  consecutive time steps to factorize:  $\mathbb{P}(\text{broken in } t \text{ time steps}) = \mathbb{P}(\text{broken in 1 time step})^t$ .

In Fig. 4 we present in detail the behavior in up to three consecutive time steps of a multiplexed network and a

multiplexed repeater chain with repairing. As previously, the chain consists of  $M = 6$  edges and for both topologies we have a multiplicity of  $N = 3$  and a repairing time of  $\tau = 7$ . The total state of each of the networks can assume two values,  $S = 0$  for "not working" and  $S = 1$  for "working". The analytical results (see Appendix D) for this random variable allow to calculate various correlations at different times.

We first consider the normalized temporal correlation  $\text{Cor}(t_a, t_b) = [\langle S(t_a)S(t_b) \rangle - \langle S(t_a) \rangle \langle S(t_b) \rangle] / [\sigma(S(t_a))\sigma(S(t_b))]$  for two consecutive time steps  $(t_1, t_2)$  or with one time step in between  $(t_1, t_3)$ ; where  $\sigma(S(t_x))$  denotes the standard deviation. Then, we consider two established measures of genuine tripartite correlation: The first one is the joint cumulant [50], which for three random variables  $A, B, C$  is defined as  $C_3 = |\langle ABC \rangle - \langle A \rangle \langle BC \rangle - \langle B \rangle \langle AC \rangle - \langle C \rangle \langle AB \rangle + 2\langle A \rangle \langle B \rangle \langle C \rangle|$ . If the joint cumulant is nonzero, then none of the random variables is independent from the other two. The second measure of tripartite correlations is based on exponential families and an extension of the multi-information [51–53]. The Kullback-Leibler distance  $D(P||Q) = \sum_j p_j \log(p_j/q_j)$  describes how surprising the probability distribution  $P$  is, if one has expected  $Q$ . Then, the correlation measure  $D_3$  of a three-variable distribution is given by the minimal distance to all probability distributions  $Q \in \mathcal{E}_2$  which are thermal states of two-body Hamiltonians, that is  $D_3(P) = \inf_{Q \in \mathcal{E}_2} D(P||Q)$ . This describes genuine three-party correlations and is used in the analysis of complex systems [51].

Looking at the results in Fig. 4 the first observation is that the repeater chain shows for smaller breaking probabilities  $p_{\downarrow}$  a non-Markovian behavior compared to the network. This is somewhat intuitive: The network is more robust to breaking, so if a complete failure rarely happens, it is more probable that the network is broken for a few time steps in sequence than in random time steps. Second, the joint cumulant  $C_3$  tends to zero if the network is equally often broken as functional. Around this point the correlation measure  $D_3$  reaches its maximum. Third, every correlation measure tends to 0 for high  $p_{\downarrow}$ , since in that case the systems remain broken most of the time.

*Applications in entanglement distribution.*— Having discussed the purely classical behavior of the technical devices in a multiplexed network, we want to use our results to derive improvements for quantum protocols run on these classical setups. We consider entanglement generation and subsequent quantum key distribution with quantum repeaters. Here, one tries to generate long-distance entangled links by first creating shorter entangled links between repeater stations and then connecting them via Bell measurements. One problem in these schemes is that the quality of existing entangled links decreases when

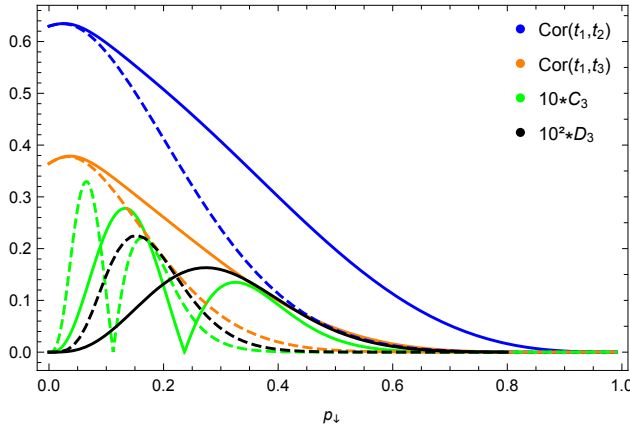


FIG. 4. Four different correlation measures demonstrating non-Markovian effects in the temporal behaviour of two network models. Solid lines show the results for the network in Fig. 3, the dashed lines for a repeater chain similar to Fig. 1(a). See text for details.

stored, due to decoherence. These weakly entangled links do not lead to high-fidelity long-range entanglement anymore and block the generation of fresh entangled pairs, so it may be useful to restrict the duration of an entanglement generation attempt by a cut-off time and erase all created links after this time [14, 54]. The cut-off time should be chosen in such a way that the secret-key rate achieved by this protocol is optimal [28, 32, 55].

We aim to find a strategy for optimizing the cutoff time for the network in Fig. 3 without multiplexing and for a chain of  $M = 6$  edges with multiplicity  $N = 3$ . We assume two different time scales; on the longer time scale devices break and are repaired, on top of that and on a much shorter timescale entanglement is probabilistically distributed according to the protocol above. We simulate the repeater protocol on all possible functional configurations of the network (the chain) and take the weighted average of the resulting secret-key rates using the probabilities for the configurations calculated by our approach above. For the simulation, we assume the Bell measurements to be perfect and use as simulation parameter the entanglement generation probability  $P_{\text{gen}} = 0.01$  and model decoherence as depolarizing noise with a coherence time  $T_{\text{coh}} = 1\text{s}$ . The duration of one time step for the quantum protocol is  $\frac{2}{3}10^{-3}\text{s}$ . For a motivation of these numbers and more details, see Ref. [56] and Appendix E.

The results of our calculations are shown in Fig. 5. In the left part the thin lines denote the secret-key rates achieved on the five different configurations of the Netherlands network (see Fig. 3 and Fig. 10 in Appendix E) depending on the chosen cut-off time. Assuming that a single edge of the network has an average up-time of  $q = 0.8$  or  $q = 0.2$  one can calculate the probabilities for the network to be in a certain configuration and from

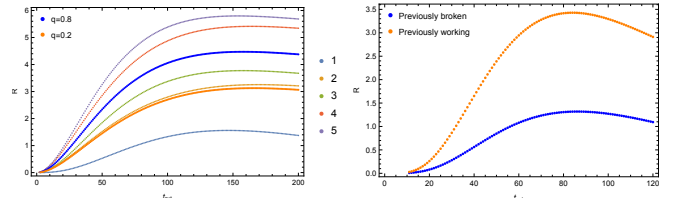


FIG. 5. Secret-key rate (bits per second) in the simplified Netherlands network (left) and on a chain with  $M = 6$  edges with  $N = 3$  (right) depending on the chosen cut-off time. The numbers refer to the different possible configurations (see Fig. 10 in Appendix E), see text for more details.

this the average secret-key rate achieved on the network. Clearly, these average key rates are lower than the one achieved on the complete network (line 5), so the classical defects of the technical devices have a significant impact on the quantum efficiency. A second observation is that the secret-key rate reaches a maximum for each configuration as well as for the complete network. So, knowing the characteristics of the technical devices leads to a better choice of the cut-off time.

In the same way, we simulated the achievable key rates on a repeater chain with  $M = 6$  edges with multiplicity  $N = 3$ . For the breaking probability we chose  $p_{\downarrow} = 1/105$  and for the repairing time  $s = 15$ . The resulting average key rates can be seen in the right part of Fig. 5. Here, we took the state of the repeater chain in the previous time step into consideration and conditioned the probabilities for the different functional configurations on whether the repeater chain was functional or broken in the previous step. One can see a clear difference between the key rates in these two different cases, which is to be expected. If the chain was functional in the time step before, then the configurations with a higher multiplicity in the edges are more probable than if the chain was broken in the previous step. So the knowledge about the previous behavior of the repeater chain can be used to choose an appropriate cut-off time for the current experiment and the breaking effects of the used technical devices can be mitigated by adapting the cut-off time of the quantum protocol to the current situation.

*Conclusion.*— We have developed analytical methods to treat failure and defects of devices in quantum networks. Our approach can be used to study temporal correlations arising from failure-and-repair mechanisms. Based on our results it is possible to study the effects of noise arising on the quantum level, resulting in criteria for optimal cut-off time.

While our methods were developed in the quantum network paradigm, it seems promising to adapt them to other examples of quantum technologies. A concrete example are segmented ion traps [57, 58]. Here, ions are shuffled on a chip from one interaction zone to the other to build quantum circuits with high fidelity. Failures of

interaction or shuffling procedures can directly be modeled with our approach and consequently the design of these ion traps can be optimized. On a more fundamental level, our results can be used to optimize entanglement distribution in networks [36, 59] as well as multipartite cryptographic protocols [60]. This will help to understand multiparticle quantum correlations as a fundamental phenomenon in nature.

*Acknowledgments.*— We thank Jan L. Bönsel, Austin Collins, Antariksha Das, Kian van der Enden, Tim

Hebenstreit, Patrick Huber, Brian Kennedy, Peter van Loock, and Fabian Zickgraf for discussions. This work was supported by the Deutsche Forschungsgemeinschaft (DFG, German Research Foundation, project numbers 447948357 and 440958198), the Sino-German Center for Research Promotion (Project M-0294), the ERC (Consolidator Grant 683107/TempoQ), the German Ministry of Education and Research (Project QuKuK, BMBF Grant No. 16KIS1618K) and the Dutch National Growth Fund, as part of the Quantum Delta NL program. LV thanks the Stiftung der Deutschen Wirtschaft.

## APPENDIX A: RELIABILITY THEORY FOR REPEATER CHAINS

In this Appendix we want to describe how one can apply reliability theory to repeater chains. First, we give a short introduction to the basics of reliability theory and the main quantities. Second, we derive some results for the easiest network structure, the repeater chain. We start by considering a single connection and then an edge or block, which consists of  $N$  parallel connections. Here we differentiate between a block consisting of  $N$  initially perfect connections and  $N$  connections which may be broken in the beginning with probability  $1 - p$ . Finally, these blocks of connections are combined to a chain. All the results are purely analytical.

### A1: Basics of Reliability Theory

The *reliability function*  $S(t)$  describes the probability that a system fails after a certain time  $t$  and is functional up to this point. If  $T$  is the random variable describing the failure time of the system then

$$S(t) = \mathbb{P}(T > t). \quad (4)$$

Using the *cumulative distribution function*

$$F(t) = \mathbb{P}(T \leq t) \quad (5)$$

one can express the reliability function as

$$S(t) = 1 - \mathbb{P}(T \leq t) = 1 - F(t). \quad (6)$$

The *failure rate* of the system is given by the logarithmic derivative of the reliability function

$$\mu(t) = -\frac{d}{dt} \ln S(t) = -\frac{1}{S(t)} \frac{d}{dt} S(t) = \frac{1}{S(t)} \frac{d}{dt} F(t). \quad (7)$$

Sometimes it is easier to express the failure rate using the *probability density function*

$$f(t) = \frac{d}{dt} F(t) = -\frac{d}{dt} S(t). \quad (8)$$

It then holds

$$\mu(t) = \frac{f(t)}{S(t)}. \quad (9)$$

### A2: Results for Repeater Chains

One block consists of a fixed number of  $N$  parallel connections. Each of these connections can be functional or broken. The block has a *flux* of  $f$ , if at least  $f$  of the  $N$  connections are functional. We want to calculate the probability to have a certain flux  $f$  depending on the time  $t$ . The calculation follows the strategy of Gavrilov and Gavrilova [38], with some modifications to avoid the underlying implicit assumption of small time scales (see also Ref. [49]). The important difference is that in their calculations a block fails if all links are destroyed. In our calculation the block "fails", if  $N - (f - 1)$  connections are destroyed, because then a flux of  $f$  is not possible anymore.

### A2.1: A single connection

A single connection has a fixed failure rate  $\mu(t) = k = \text{const}$ , so it decays exponentially. Let  $T$  be the random variable which describes the failure time of a single connection. For the exponential distribution it holds

$$S(1, k, t) := \mathbb{P}(T > t) = 1 - F(t) = e^{-kt} =: \alpha \quad (10)$$

and

$$F(1, k, t) := \mathbb{P}(T \leq t) = 1 - e^{-kt} = 1 - \alpha. \quad (11)$$

Note that it holds:

$$\frac{d\alpha}{dt} = -ke^{-kt} = -k\alpha. \quad (12)$$

### A2.2: A block with initially perfect connections

One block consists of a fixed number of connections  $N$ . In the beginning all  $N$  of these connections are functional. We want to calculate the probability to have a certain flux  $f$  depending on the time  $t$ .

**Proposition 1.** *Given a block of  $N$  working connections which each fail according to a constant failure rate  $\mu(t) = k$  the reliability function of the block  $b$  for a flux  $f$  at time  $t$  is given by*

$$S_b^f(N, k, t) = \sum_{i=0}^{N-f} \binom{N}{i} [1 - \alpha]^i \alpha^{N-i} \quad (13)$$

and the failure rate is given by

$$\mu_b^f(N, k, t) = \frac{k f \binom{N}{f} [1 - \alpha]^{N-f} \alpha^f}{\sum_{i=0}^{N-f} \binom{N}{i} [1 - \alpha]^i \alpha^{N-i}} \quad (14)$$

with  $\alpha = e^{-kt}$ .

*Proof.* Denote the failure time of the block with  $T_b$  and the failure time of the  $i$ -th connection with  $T_i$ . The failure times of the connections are iid, so the probability for the failure of  $i$  arbitrary connections is the same as for the connections  $1, \dots, i$ . The block fails in time  $T_b \leq t$  and has therefore a flux  $\leq f - 1$ , if at least  $N - (f - 1)$  of the links fail before  $t$ :

$$\begin{aligned} F_b^f(N, k, t) &= \mathbb{P}(T_b \leq t) \\ &= \sum_{i=N-(f-1)}^N \binom{N}{i} \mathbb{P}(T_1, \dots, T_i \leq t) \mathbb{P}(T_{i+1}, \dots, T_N > t) \\ &= \sum_{i=N-(f-1)}^N \binom{N}{i} \mathbb{P}(T_1 \leq t) \cdots \mathbb{P}(T_i \leq t) \mathbb{P}(T_{i+1} > t) \cdots \mathbb{P}(T_N > t) \\ &= \sum_{i=N-(f-1)}^N \binom{N}{i} [F(1, k, t)]^i [S(1, k, t)]^{N-i} \\ &= \sum_{i=N-(f-1)}^N \binom{N}{i} [1 - \alpha]^i \alpha^{N-i} \\ &= \sum_{i=0}^N \binom{N}{i} [1 - \alpha]^i \alpha^{N-i} - \sum_{i=0}^{N-f} \binom{N}{i} [1 - \alpha]^i \alpha^{N-i} \\ &= 1 - \sum_{i=0}^{N-f} \binom{N}{i} [1 - \alpha]^i \alpha^{N-i}. \end{aligned} \quad (15)$$

The reliability function is then given by

$$S_b^f(N, k, t) = \mathbb{P}(T_b > t) = 1 - F_b^f(N, k, t) = \sum_{i=0}^{N-f} \binom{N}{i} [1 - \alpha]^i \alpha^{N-i}. \quad (16)$$

For the failure rate we calculate first the probability density function

$$f_b^f(N, k, t) = -\frac{d}{dt} S_b^f(N, k, t) \quad (17)$$

$$\begin{aligned} &= -\frac{d\alpha}{dt} \frac{d}{d\alpha} \sum_{i=0}^{N-f} \binom{N}{i} [1 - \alpha]^i \alpha^{N-i} \\ &= k\alpha \left[ \sum_{i=0}^{N-f} \binom{N}{i} [1 - \alpha]^i (N - i) \alpha^{N-i-1} + \sum_{i=1}^{N-f} \binom{N}{i} (-1)i [1 - \alpha]^{i-1} \alpha^{N-i} \right] \\ &= k\alpha \left[ \sum_{i=0}^{N-f} \binom{N}{i} (N - i) [1 - \alpha]^i \alpha^{N-i-1} - \sum_{i=0}^{N-f-1} \binom{N}{i+1} (i+1) [1 - \alpha]^i \alpha^{N-(i+1)} \right]. \end{aligned} \quad (18)$$

Then it holds

$$\binom{N}{i+1} (i+1) = \frac{N!}{(i+1)!(N-i-1)!} (i+1) = \frac{N!}{i!(N-i)!} (N-i) = \binom{N}{i} (N-i) \quad (19)$$

and therefore

$$\begin{aligned} f_b^f(N, k, t) &= k\alpha \left[ \sum_{i=0}^{N-f} \binom{N}{i} (N - i) [1 - \alpha]^i \alpha^{N-i-1} - \sum_{i=0}^{N-f-1} \binom{N}{i} (N - i) [1 - \alpha]^i \alpha^{N-(i+1)} \right] \\ &= k\alpha \binom{N}{N-f} [N - (N-f)] [1 - \alpha]^{N-f} \alpha^{N-(N-f)-1} \\ &= kf \binom{N}{f} [1 - \alpha]^{N-f} \alpha^f. \end{aligned} \quad (20)$$

The failure rate is then the fraction of the probability density function and the reliability:

$$\begin{aligned} \mu_b^f(N, k, t) &= \frac{f_b^f(N, k, t)}{S_b^f(N, k, t)} \\ &= \frac{kf \binom{N}{f} [1 - \alpha]^{N-f} \alpha^f}{\sum_{i=0}^{N-f} \binom{N}{i} [1 - \alpha]^i \alpha^{N-i}} \\ &= \frac{kf \binom{N}{f} [\alpha^{-1} - 1]^{N-f}}{\sum_{i=0}^{N-f} \binom{N}{i} [\alpha^{-1} - 1]^i}. \end{aligned} \quad (21)$$

□

### A2.3: A block with probabilistic connections

In this model one block consists of a fixed number of connections  $N$ . In the beginning, only  $n$  of these connections are functional. The number  $n$  depends on some probability distribution  $q_n$  with  $\sum_{n=0}^N q_n = 1$ , e. g., the binomial distribution  $q_n = \binom{N}{n} p^n (1-p)^{N-n}$ . The binomial distribution describes the case where each single connection is functional with probability  $p$ . In general the distribution  $q_n$  can be arbitrary.

We want to calculate the probability to have a certain flux  $f$  depending on the time  $t$ .

**Proposition 2.** *Given a block of  $N$  connections of which  $n$  connections are working in the beginning with probability  $q_n$  and denote the probability distribution by  $Q = \{q_n\}$ . Each working connection fails according to a constant failure*

rate  $\mu(t) = k$ . Then the reliability function of the block for a flux  $\mathfrak{f}$  at time  $t$  is given by

$$S_b^{\mathfrak{f}}(N, Q; k, t) = \sum_{n=\mathfrak{f}}^N q_n S_b^{\mathfrak{f}}(n, k, t) \quad (22)$$

and the failure rate is given by

$$\mu_b^{\mathfrak{f}}(N, Q; k, t) = \frac{1}{S_b^{\mathfrak{f}}(N, Q; k, t)} \sum_{n=\mathfrak{f}}^N q_n \mu_b^{\mathfrak{f}}(n, k, t) S_b^{\mathfrak{f}}(n, k, t). \quad (23)$$

*Proof.* Using the law of total probability it holds for the reliability

$$S_b^{\mathfrak{f}}(N, Q; k, t) = \mathbb{P}(T_b > t) = \sum_{n=\mathfrak{f}}^N q_n S_b^{\mathfrak{f}}(n, k, t). \quad (24)$$

For the failure rate it then follows

$$\begin{aligned} \mu_b^{\mathfrak{f}}(N, Q; k, t) &= -\frac{1}{S_b^{\mathfrak{f}}(N, Q; k, t)} \frac{d}{dt} \sum_{n=\mathfrak{f}}^N q_n S_b^{\mathfrak{f}}(n, k, t) \\ &= \frac{1}{S_b^{\mathfrak{f}}(N, Q; k, t)} \sum_{n=\mathfrak{f}}^N q_n S_b^{\mathfrak{f}}(n, k, t) \left[ -\frac{1}{S_b^{\mathfrak{f}}(n, k, t)} \frac{d}{dt} S_b^{\mathfrak{f}}(n, k, t) \right] \\ &= \frac{1}{S_b^{\mathfrak{f}}(N, Q; k, t)} \sum_{n=\mathfrak{f}}^N q_n S_b^{\mathfrak{f}}(n, k, t) \mu_b^{\mathfrak{f}}(n, k, t). \end{aligned} \quad (25)$$

□

In Ref. [38] they use at this point implicitly an approximation for small time scales by calculating the failure rate for a flux of  $\mathfrak{f} = 1$  without the weights  $\frac{S_b^1(n, k, t)}{S_b^1(N, Q; k, t)}$ :

$$\mu_b^1(N, Q; k, t) = \sum_{n=1}^N \tilde{q}_n \mu_b^1(n, k, t). \quad (26)$$

The probabilities  $\tilde{q}_n$  are normalized, such that the probability  $\tilde{q}_0$  for a failure right in the beginning is 0. In this case, the reliabilities  $S_b^1(N, Q; k, 0) = 1$  and  $S_b^1(n, k, 0) = 1$  cancel for  $t = 0$  (since the device is surely functional in the beginning). However, for larger times  $t$  the weights become relevant and lead to a very different behavior than in Ref. [38].

#### A2.4: A chain

**Proposition 3.** Given a chain of  $M$  blocks with respective reliability functions  $S_{b_j}(t)$  and failure rates  $\mu_{b_j}(t)$ ,  $j = 1, \dots, M$ , then the reliability function and failure rate of the whole chain are given by the product or sum, respectively:

$$S_{\text{chain}} = \prod_{j=1}^M S_{b_j}(t) \quad \text{and} \quad \mu_{\text{chain}}(t) = \sum_{j=1}^M \mu_{b_j}(t). \quad (27)$$

*Proof.* Let  $T_{\text{chain}}$  be the failure time of the chain and  $T_{b_j}$  the failure time of block  $j = 1, \dots, M$ . The failure times of the blocks are independent, but not necessarily identically distributed. The whole chain fails if at least one of the blocks fails. Therefore it holds

$$\begin{aligned} S_{\text{chain}}(t) &= \mathbb{P}(T_{\text{chain}} > t) = \mathbb{P}(T_{b_1}, \dots, T_{b_M} > t) \\ &= \prod_{j=1}^M \mathbb{P}(T_{b_j} > t) \\ &= \prod_{j=1}^M S_{b_j}(t) \end{aligned} \quad (28)$$

and

$$\begin{aligned}\mu_{\text{chain}}(t) &= -\frac{d}{dt} \ln S_{\text{chain}}(t) = -\frac{d}{dt} \ln \prod_{j=1}^M S_{b_j}(t) \\ &= \sum_{j=1}^M \left( -\frac{d}{dt} \ln S_{b_j}(t) \right) = \sum_{j=1}^M \mu_{b_j}(t).\end{aligned}\quad (29)$$

□

If the blocks are all iid, then it simply holds

$$S_{\text{chain}}(t) = [S_b(t)]^M \quad (30)$$

and

$$\mu_{\text{chain}}(t) = M\mu_b(t). \quad (31)$$

## APPENDIX B: PROBABILITIES IN MORE COMPLEX TOPOLOGIES

To calculate the probabilities for a network to be functional or not, one has to consider the different possible paths in this network that lead to a resulting connection from one point of the network to another. This type of probabilities can e.g. be computed using the principle of inclusion and exclusion. Another easier and more clear option is the use of indicator functions. This idea can, e.g., be found in Ref. [61]. We use indicator functions of the type

$$\mathbb{1}_X = \begin{cases} 1, & \text{if } X \text{ is functional,} \\ 0, & \text{if } X \text{ is broken.} \end{cases} \quad (32)$$

Then it holds

$$\mathbb{P}(X \text{ is functional}) = 1 \times \mathbb{P}(X \text{ is functional}) + 0 \times \mathbb{P}(X \text{ is broken}) = \mathbb{E}[\mathbb{1}_X]. \quad (33)$$

So to calculate the probability for the whole system to be functional we first calculate the indicator function and then take the average value.

If  $A$  and  $B$  are two components, which are connected in series to get the larger component  $X$ , then  $X$  is functional iff  $A$  and  $B$  are functional. The indicator function of  $X$  then reads as

$$\begin{aligned}\mathbb{1}_X &= \begin{cases} 1, & \text{if } \mathbb{1}_A = \mathbb{1}_B = 1, \\ 0, & \text{else} \end{cases} \\ &= \mathbb{1}_A \times \mathbb{1}_B\end{aligned}\quad (34)$$

and the probability is therefore (since  $A$  and  $B$  are independent)

$$\mathbb{P}(X \text{ is functional}) = \mathbb{E}[\mathbb{1}_X] = \mathbb{E}[\mathbb{1}_A] \times \mathbb{E}[\mathbb{1}_B] = \mathbb{P}(A \text{ is functional}) \times \mathbb{P}(B \text{ is functional}). \quad (35)$$

If the components are connected in parallel, the indicator function of  $X$  instead reads

$$\begin{aligned}\mathbb{1}_X &= \begin{cases} 1, & \text{if } \mathbb{1}_A = 1 \text{ or } \mathbb{1}_B = 1, \\ 0, & \text{else} \end{cases} \\ &= 1 - (1 - \mathbb{1}_A) \times (1 - \mathbb{1}_B)\end{aligned}\quad (36)$$

and the probability is (since  $A$  and  $B$  are independent)

$$\mathbb{P}(X \text{ is functional}) = \mathbb{E}[\mathbb{1}_X] = 1 - (1 - \mathbb{E}[\mathbb{1}_A]) \times (1 - \mathbb{E}[\mathbb{1}_B]) = 1 - \mathbb{P}(A \text{ is broken}) \times \mathbb{P}(B \text{ is broken}). \quad (37)$$

The idea to use indicator functions instead of probabilities becomes more interesting when considering more difficult networks. For the simple square network with one diagonal connection (see picture 6; the square contains the

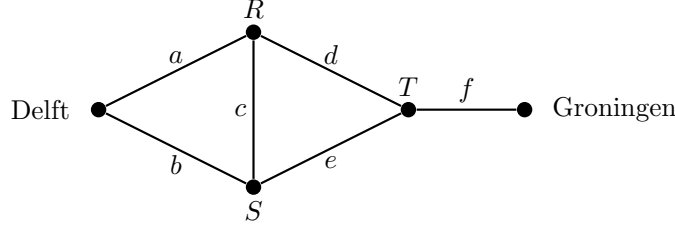


FIG. 6. Simplification of the network in Ref. [43] from Delft to Groningen; the network consists of three components in series: a square network (with one diagonal connection  $c$ ) from Delft up to node  $T$ , the node  $T$  itself and a single link  $f$  to Groningen.

connections from Delft to the node  $T$ , including nodes  $R$  and  $S$ ) the indicator function becomes

$$\begin{aligned} \mathbb{1}_{\text{square}} &= \begin{cases} 1, & \text{if } \mathbb{1}_{aRd} = 1 \text{ or } \mathbb{1}_{aRcSe} = 1 \text{ or } \mathbb{1}_{bSe} = 1 \text{ or } \mathbb{1}_{bScRd} = 1 \\ 0, & \text{else} \end{cases} \\ &= 1 - (1 - \mathbb{1}_{aRd}) \times (1 - \mathbb{1}_{aRcSe}) \times (1 - \mathbb{1}_{bSe}) \times (1 - \mathbb{1}_{bScRd}), \end{aligned} \quad (38)$$

where  $\mathbb{1}_{aRd}$  is the short notation for  $\mathbb{1}_a \mathbb{1}_R \mathbb{1}_d$ . Using the fact that  $\mathbb{1}^2 = \mathbb{1}$ , one obtains

$$\begin{aligned} \mathbb{1}_{\text{square}} &= \mathbb{1}_{aR}(\mathbb{1}_d + \mathbb{1}_{cSe} - \mathbb{1}_{decS}) + \mathbb{1}_{bS}(\mathbb{1}_e + \mathbb{1}_{cRd} - \mathbb{1}_{ecdR}) \\ &\quad - \mathbb{1}_{abRS}(\mathbb{1}_{de} + \mathbb{1}_{cd} + \mathbb{1}_{ce} - 2 \times \mathbb{1}_{ced}). \end{aligned} \quad (39)$$

Note that all the indicator functions in the products are independent. Therefore one can just calculate the average value of each single term to get the average value of  $\mathbb{1}_{\text{square}}$ . In the special case that the edges and nodes all have the same respective probabilities for failures  $\mathbb{P}(\text{edge is broken}) = e$  and  $\mathbb{P}(\text{node is broken}) = n$ , the probability for the network to be functional is simply

$$\begin{aligned} \mathbb{P}(\text{square is functional}) &= \mathbb{E}[\mathbb{1}_{\text{square}}] = en(e + e^2n - e^3n) + en(e + e^2n - e^3n) \\ &\quad - e^2n^2(e^2 + e^2 + e^2 - 2 \times e^3) \\ &= 2e^2n + e^3n^2(2 - 5e + 2e^2). \end{aligned} \quad (40)$$

The network in Ref. [43] from Delft to Groningen is then a series of a square network, a node  $T$  and a single link  $f$ . Therefore the indicator function for the connection from Delft to Groningen reads as

$$\mathbb{1}_X = \mathbb{1}_{\text{square}} \times \mathbb{1}_T \times \mathbb{1}_f. \quad (41)$$

### APPENDIX C: APPLICATIONS OF THE THEORY: CHAINS AND NETWORKS

The methods described in the two chapters before are now demonstrated on two different examples. In Appendix A we saw that there is a difference between the following two models:

- (a) Each edge has a multiplicity of  $N$ , where every physical connection works perfectly in the beginning; however, the connections are affected by an exponential decay with failure rate  $\mu$ .
- (b) Each edge has a multiplicity of  $N'$ , where each physical connection is not working in the beginning with a certain probability  $p$ ; the connections are also affected by an exponential decay with failure rate  $\mu'$ .

In Fig. 7 we plot now the two resulting reliability functions and failure rates for these two models and two different topologies. The first topology is a chain consisting of  $M = 6$  edges compared to the second topology of the network in Fig. 6, which also consists of 6 edges. The results for the network are obtained using indicator functions as described in the last chapter. There are several observations. First, the reliability functions according to model (b) have a negative offset at  $t = 0$ . This should be expected, as there is a nonzero probability that the whole system is not functional right from the start as each connection is only functional with probability  $1 - p$ . However, the offset is smaller in the case of the network since there are more possible end-to-end paths. Analogous, the failure rates for model (b) do not start at 0 for  $t = 0$ . A second observation shows, that the two models behave the same way in

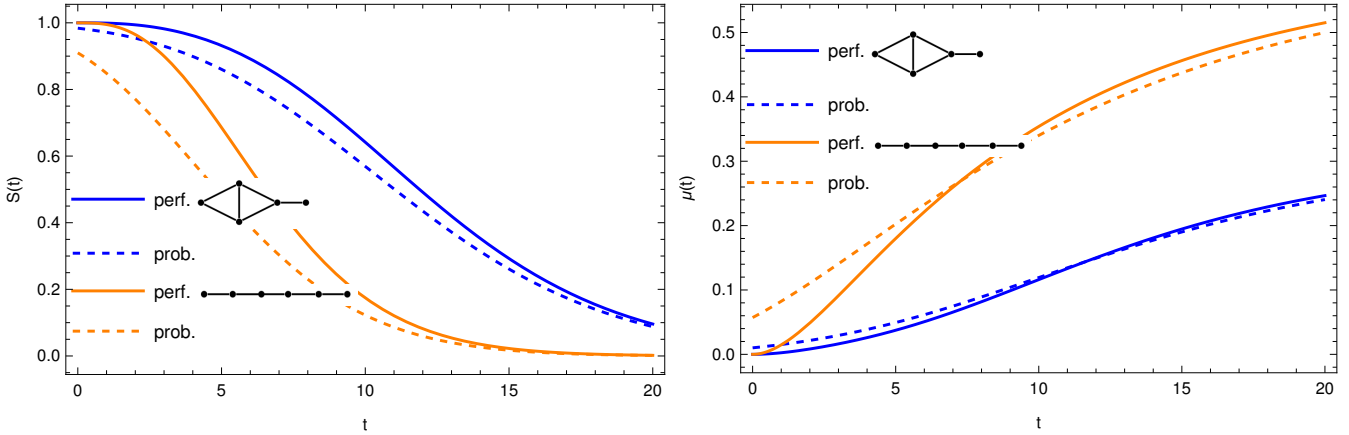


FIG. 7. Reliability function  $S(t)$  and failure rate  $\mu(t)$  of a network or chain depending on the time  $t$ ; the solid lines denote the results for model (a), where each edge has a multiplicity of  $N = 3$ ; the dashed lines denote the results for model (b), where each edge has a multiplicity of  $N' = 6$  and a initial failure probability of  $p = 1/2$ .

the long run. If the single connections started to fail, at some point there is not much difference between an initially broken connection and a connection which broke in the last few minutes. However, in the short time range, model (a) performs better. The last observation concerns the different topologies. It is not surprising that the network shows a more stable behavior, that is a slower decreasing reliability and a slower increasing failure rate. The chain will fail as soon as one of the edges fails, the network however is robust to the failure of up to three edges as long as there exists still a path from end to end.

#### APPENDIX D: REPAIRING OF BROKEN DEVICES AND RESULTING NON-MARKOVIAN EFFECTS

In the following chapter we want to model the behavior of a network in which the connections not only break after some time, but also get repaired. We assume that the repairing takes some time. Mathematically speaking, the connections can break in each time step with probability  $p_\downarrow$ , e.g. the breaking is geometrically distributed. If a connection is broken it gets repaired after  $\tau$  time steps. After this repairing time, the repaired connection can either break directly again with probability  $p_\downarrow$  or stay functional with probability  $1 - p_\downarrow$ . Note that this means that it is not guaranteed that after  $\tau$  time steps the connection is functional again, it can well happen that it is broken for  $2\tau$  or even more multiples of  $\tau$ .

We want to calculate the probability that a block of  $N$  connections or a network behaves in a certain way in  $t$  arbitrarily chosen consecutive time steps. To reach this goal we first calculate the probabilities for a single connection to behave in a certain way in up to three consecutive time steps. Then we show how these probabilities can be used to describe the behavior of a block of  $N$  connections and more complex networks.

##### D1: A single connection

We start by calculating all needed probabilities for a single connection.

**Proposition 4.** *The probability for a single connection with failure probability  $p_\downarrow$  and repairing time  $\tau$  to be broken in an arbitrarily chosen time step is given by*

$$p_{\text{eff}}^b = \frac{\tau}{1/p_\downarrow - 1 + \tau}. \quad (42)$$

*Proof.* Since the breaking of a connection is geometrically distributed, the first break will happen on average in time step  $1/p_\downarrow$ . Thus, the connection is on average functional for  $1/p_\downarrow - 1$  time steps and then broken for another  $\tau$  time steps. The probability that the connection is broken in an arbitrarily chosen time step is thus

$$p_{\text{eff}}^b = \frac{\tau}{1/p_\downarrow - 1 + \tau} \quad (43)$$

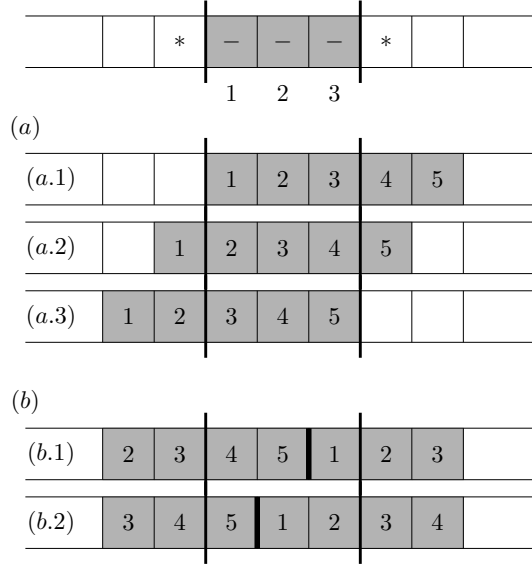


FIG. 8. Possible states of a connection with repairing time  $\tau = 5$  to be broken in  $t = 3$  arbitrarily chosen consecutive time steps; (a) if the first of the consecutive time steps coincides with one of the first  $\tau - t + 1 = 3$  broken steps of the connection, the connection is broken throughout the three consecutive time steps; (b) if the first of the consecutive time steps coincides with one of the last  $t - 1 = 2$  broken steps of the connection, then the connection has to break again directly after being repaired to remain broken through the three consecutive time steps.

and the probability that the connection is functional is

$$p_{\text{eff}}^f = \frac{1/p_{\downarrow} - 1}{1/p_{\downarrow} - 1 + \tau} = 1 - p_{\text{eff}}^b. \quad (44)$$

□

In the next step we want to calculate the probability that a single connection is broken in not only one arbitrarily chosen time step but instead in  $1 \leq t \leq \tau$  consecutive arbitrarily chosen time steps.

**Proposition 5.** *The probability for a single connection with failure probability  $p_{\downarrow}$  and repairing time  $\tau$  to be broken in  $1 \leq t \leq \tau$  arbitrarily chosen consecutive time steps is given by*

$$m(t) = p_{\text{eff}}^b \left( 1 - \frac{t-1}{\tau} (1 - p_{\downarrow}) \right). \quad (45)$$

*Proof.* The probability for the connection to be broken in  $t$  consecutive time steps  $m(t)$  can be calculated in a similar way as in Proposition 4 (see also Fig. 8). We saw there that a connection is on average functional for  $1/p_{\downarrow} - 1$  time steps and then broken for another  $\tau$  time steps. Thus, the first of the  $t$  consecutive time steps has to coincide with one of the  $\tau$  broken steps of the device. If it coincides with one of the first  $\tau - t + 1$  broken steps of the device then the device remains surely broken for the following  $t - 1$  time steps. If it coincides with one of the  $t - 1$  last broken steps of the device then the device has to break again directly after being repaired to stay broken in the remaining  $t - 1$  consecutive time steps. This happens with probability  $p_{\downarrow}$ . One therefore gets

$$m(t) = \frac{\tau - t + 1}{1/p_{\downarrow} - 1 + \tau} \times 1 + \frac{t-1}{1/p_{\downarrow} - 1 + \tau} \times p_{\downarrow} \quad (46)$$

$$= \frac{\tau}{1/p_{\downarrow} - 1 + \tau} \left( 1 - \frac{(t-1)(1-p_{\downarrow})}{\tau} \right). \quad (47)$$

□

We now use the short notation + or - if the respective system is functional or not functional in a given time step and \* if the state of the system is arbitrary or not known. The probability that a connection is broken in 3 consecutive

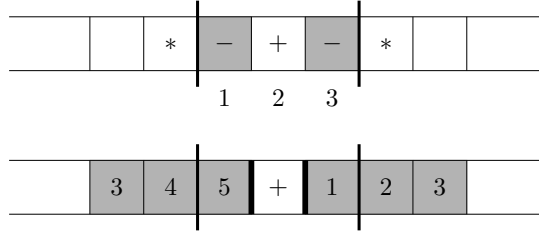


FIG. 9. Possible states of a connection with repairing time  $\tau = 5$  which is broken, functional and broken again in  $t = 3$  arbitrarily chosen consecutive time steps; the first of the consecutive time steps has to coincide with the last of the broken steps of the connection; after being repaired the connection has to stay functional and then break again.

time steps would then be denoted by  $m(3) = p_c^{---}$  and the effective probability for 1 time step by  $p_{\text{eff}}^b = m(1) = p_c^-$ . For a single connection all probabilities  $p_c^{i_1, \dots, i_t}$  for the behavior  $i_1, \dots, i_t$  in  $t$  consecutive time steps can be calculated in the same fashion as above by counting all possible states of the connection. One last example for this type of calculation, the probability  $p_c^{-+}$ , is given below, since this probability is needed in the next subsection treating blocks of  $N$  connections.

**Proposition 6.** *The probability for a single connection with failure probability  $p_\downarrow$  and repairing time  $\tau$  to be broken, functional and broken again in 3 arbitrarily chosen consecutive time steps is given by*

$$p_c^{-+} = \frac{(1 - p_\downarrow)p_\downarrow}{1/p_\downarrow - 1 + \tau}. \quad (48)$$

*Proof.* The connection is on average functional for  $1/p_\downarrow - 1$  time steps and then broken for another  $\tau$ . For the connection to be broken, functional and broken again the first of the three consecutive time steps has to coincide with the last time step of the repairing time (see figure 9). This happens with probability  $\frac{1}{1/p_\downarrow - 1 + \tau}$ . After that, the connection stays functional with probability  $1 - p_\downarrow$  and breaks again with probability  $p_\downarrow$ . All in all it holds

$$p_c^{-+} = \frac{1}{1/p_\downarrow - 1 + \tau} \times (1 - p_\downarrow) \times p_\downarrow. \quad (49)$$

□

Note that probabilities of the type  $p_c^{-*}$  are given by the sum of all possible cases:

$$p_c^{-*} = p_c^{-+} + p_c^{--}. \quad (50)$$

## D2: A block of $N$ connections

To calculate now the probabilities for a block of  $N$  connections to be in a certain state in  $t$  consecutive time steps we use two main ingredients. First, we notice that a block is broken iff every single connection is broken. So all probabilities for combinations of  $-$  and  $*$  can be directly calculated by raising the respective probability for a single connection to the power of  $N$ . For example it holds

$$p^{---} = (p_c^{---})^N \quad \text{and} \quad p^{-*} = (p_c^{-*})^N. \quad (51)$$

Secondly, we can start computing the probabilities for  $t = 1$  arbitrary time step and then recursively calculate the still missing probabilities for more time steps (the ones which contain at least one  $+$ ) by using the marginals. For example it holds  $p^{+-} + p^{-} = p^{*-} = p^-$ . For 1 time step we get

$$p^+ = 1 - p^-, \quad (52)$$

for  $t = 2$  time steps

$$p^{+-} = p^{-+} = p^- - p^{--}, \quad (53)$$

$$p^{++} = p^+ - p^{+-}, \quad (54)$$

and for  $t = 3$  time steps

$$p^{+--} = p^{--+} = p^{--} - p^{---}, \quad (55)$$

$$p^{-+-} = p^{-*-} - p^{---}, \quad (56)$$

$$p^{-++} = p^{++-} = p^{-+} - p^{-+-}, \quad (57)$$

$$p^{+-+} = p^{+-} - p^{+--}, \quad (58)$$

$$p^{+++} = p^{++} - p^{++-}. \quad (59)$$

### D3: A chain or network

To calculate the probability for a chain or a network to be in a given state in  $t$  consecutive time steps we use the approach explained in Appendix . If the functionality of the system is described by the random variable  $X$  we include the time dependence by describing the system in the time steps  $1, \dots, t$  by the random variables  $X_1, \dots, X_t$ . The system is then functional in time step  $k$ , iff  $\mathbb{1}_{X_k} = 1$ . The system being functional in the first step, in an arbitrary state in the second step and being broken in the third step can, e.g., be expressed by the indicator function

$$\mathbb{1}_S^{+*-} = \mathbb{1}_{X_1} \times 1 \times (1 - \mathbb{1}_{X_3}) \quad (60)$$

and the according probability can be calculated using

$$p_S^{+*-} = \mathbb{P}(X_1 = 1, X_2 \in \{0, 1\}, X_3 = 0) = \mathbb{E}[\mathbb{1}_{X_1} \times 1 \times (1 - \mathbb{1}_{X_3})] \quad (61)$$

If  $\mathbb{1}_X$  is an expression containing different indicator functions, then each of these needs to get indexed by the time steps. So, e.g., two components in series in time step  $k$  are described by  $\mathbb{1}_{X_k} = \mathbb{1}_{A_k} \times \mathbb{1}_{B_k}$ . The only thing one has to keep in mind is that different components (e.g.,  $A$  and  $B$ ) may be independent, but the same component in different time steps  $A_k$  and  $A_j$ ,  $j \neq k$ , are not. We have to use the probabilities for a single block described in the section before. For example it holds for a block  $A$

$$\mathbb{E}[\mathbb{1}_{A_1} \mathbb{1}_{A_3}] = p^{+*+} \neq p^+ p^+ = \mathbb{E}[\mathbb{1}_{A_1}] \mathbb{E}[\mathbb{1}_{A_3}] \quad (62)$$

## APPENDIX E: DESCRIPTION OF THE MODEL AND THE NUMERICAL CALCULATIONS

In the main text of the paper, we ask whether technical devices are working or not, that is, whether we could in principle establish an entangled connection between two nodes or not. As an application, we simulated the actual generation of entangled links on such not perfectly working repeater chains and networks. In this simulation, to establish an entangled link between two far away parties, we first create shorter entangled links between repeater stations and then connect these by Bell measurements. In our model, we assume deterministic entanglement swapping. Therefore it is sufficient to create one link on each segment on the way between the two end nodes. We further assume that established links experience decoherence while waiting for other links to get established, this decoherence motivates a potential cutoff after certain time, as the entanglement in the links becomes too weak or disappears. We are interested in the secret-key rates achievable on a chain or network depending on the functionality of the technical devices. In the following, we discuss details about the simulation program (written in Python) and chosen simulation parameters.

We compute the waiting time as follows: We first simulate the waiting time for each individual connection using Monte Carlo simulation, see for example Ref. [62]. In the case of multiplexing, we determine the waiting time of a block by taking the minimum waiting time of all connections associated to that block. The waiting time of the full chain is the maximal waiting time among all blocks. In the network case, the waiting time of the full network is the waiting time of the path which gets established first.

We model memory decoherence as depolarisation noise as follows. Each entangled pair is modelled as a Werner state

$$\rho(w) = w |\Psi^-\rangle\langle\Psi^-| + (1 - w) \frac{\mathbb{I}}{4}, \quad (63)$$

where  $w$  is the visibility (or Werner parameter) and  $|\Psi^-\rangle$  is a perfect Bell state. We assume that the sources distribute maximally entangled states, i.e.,  $w = 1$ , but stored entangled states experience decoherence. At time  $t$

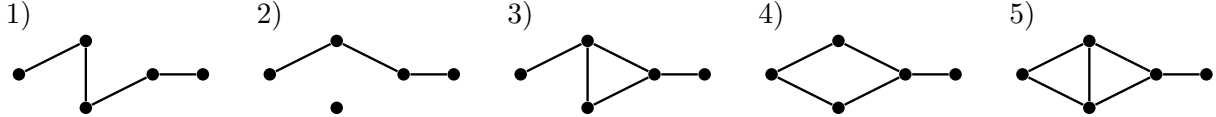


FIG. 10. Possible network configurations allowing for entanglement distribution between the end nodes for the network in the Netherlands (see Fig. 3), up to symmetries.

after establishing the entangled link, the visibility becomes  $w(t) = e^{-t/T_{coh}}$ , where  $T_{coh}$  is the coherence time of the memories. The fidelity  $F = \langle \Psi^- | \rho(w) | \Psi^- \rangle$  is given by  $F = \frac{(1+3w)}{4}$ . An entanglement swapping operation using two Werner states  $\rho(w_A), \rho(w_B)$  yields a Werner state  $\rho(w_A \times w_B)$ .

For the chosen simulation parameters we assume the distance from the source to the repeater to be  $L = 100$  km. For attenuation losses of 0.2dB/km, i.e., an attenuation length  $L_{att} \approx 22$  km, the probability to generate a link successfully is given by  $P_{gen} = e^{-\frac{L}{L_{att}}} \approx 0.01$ . The length of one time step is limited by  $t_{ts} = \frac{2}{c}L \approx \frac{2}{3}10^{-3}s$ , where  $c$  is the speed of light. We assume a memory coherence time of  $T_{coh} = 1s = 1500 \times t_{ts}$ . For a motivation of the simulation parameters, see Ref. [56].

We simulate the behaviour of a network and a chain. We consider failure of devices on a different timescale (hours or days) than link generation (seconds). Therefore we assume that for the time of one entanglement generation attempt the network or the chain has a fixed configuration of working and non-working devices. The considered network is shown in Fig. 3 and no multiplexing is used. Due to the aging process, some links might not work, so that one cannot establish entanglement with them. Using symmetries, we need to consider five different network configurations which are shown in Fig. 10.

The chain is of the type shown in Fig. 1. It consists of  $M = 6$  segments with a multiplicity of  $N = 3$ . Due to failures, we might establish entanglement on segments with lower multiplicity. Taking symmetries into account, we have 28 different functional configurations of multiplicities. This number results from taking all combinations of 1, 2 and 3 functional links per edge up to symmetry. For example, the first configurations would be (1, 1, 1, 1, 1, 1), (1, 1, 1, 1, 1, 2), (1, 1, 1, 1, 1, 3) and (1, 1, 1, 1, 2, 2), where the first three all have one functional link in the first 5 edges and 1, 2, 3 link(s) in the last edge, respectively. The last configuration has one link in the first four edges and two links in the last two edges. Note that the second configuration is symmetric to every permutation (1, 1, 1, 1, 2, 1), (1, 1, 1, 2, 1, 1) etc. of it.

We modeled  $6 \times 10^6$  data points for each configuration of the network. Here, each data point is generated by a simulation of the process of entanglement generation until success was achieved. Consequently, each data point consists of a time stamp and a fidelity of the distributed state. From the obtained data we calculate the secret-key rate  $R = r/\langle T \rangle$  of the BB84 protocol which is computed as the fraction of the secret-key fraction  $r$  and the average waiting time  $\langle T \rangle$ . We give here a short overview, for a more detailed discussion see Ref. [32]. The secret-key fraction for a Werner state with visibility  $w$  is given by

$$r(w) = \max\{0, 1 + (1 - w) \log_2 \frac{1 - w}{2} + (1 + w) \log_2 \frac{1 + w}{2}\}. \quad (64)$$

In order to characterize the effect of different cut-off times, we consider the case that the entanglement generation attempt is terminated after  $t_{cut}$  time steps. If there is, after this time, not in every edge an entangled link, then every existing link is erased and a new generation attempt is started. Let  $T$  denote the time when every entangled link exists, so that the protocol reached a successful entanglement generation attempt. Then

$$p_{cut} = \mathbb{P}(T \leq t_{cut})$$

denotes the probability that the entanglement generation was successful during  $t_{cut}$  and

$$\frac{\sum_{t=1}^{t_{cut}} t \mathbb{P}(T = t)}{p_{cut}}$$

is the average time until success during that attempt. The average time for which the cut-off procedure is repeated until the first successful attempt is reached is then geometrically distributed with  $p_{cut}$  and given by

$$t_{cut} \sum_{k=1}^{\infty} k \times p_{cut} (1 - p_{cut})^k = t_{cut} \frac{1 - p_{cut}}{p_{cut}}.$$

All in all, the average waiting time until entanglement generation is given by the sum of the time until the first successful attempt and the waiting time for that success in that attempt:

$$\langle T \rangle = t_{\text{cut}} \frac{1 - p_{\text{cut}}}{p_{\text{cut}}} + \frac{\sum_{t=1}^{t_{\text{cut}}} t \mathbb{P}(T = t)}{p_{\text{cut}}}.$$

The resulting end-to-end Werner state has then a visibility parameter  $W$  which is the product of the visibilities of the single-connection Werner states in the connected path. Its mean value is given by

$$\langle W \rangle = \frac{\sum_{t=1}^{t_{\text{cut}}} W(t) \mathbb{P}(T = t)}{p_{\text{cut}}}$$

From the obtained data we can now calculate the secret-key rates  $R_i$  for every possible functional configuration  $i$  of the network and the chain and every choice of  $t_{\text{cut}}$ . The average secret-key rate which can be achieved by this protocol on the respective topology is then given by the weighted sum of the different rates where the weights are the probabilities  $\mathbb{P}(\text{configuration } i)$  of the different configurations.

The simulation is single threaded but multiple simulations were executed in parallel. The result was obtained by running eight parallel simulations for one to two days on a computer with the following specification: Intel Core i7-4790 CPU with 3.60GHz running at 4 cores / 8 threads with 16 GB of memory available. The computation was not memory intensive. The code can be found online [63]. The computed data can be made available upon reasonable request.

---

[1] N. M. Linke, D. Maslov, M. Roetteler, S. Debnath, C. Figgatt, K. A. Landsman, K. Wright, and C. Monroe, *Proc. Natl. Acad. Sci. U.S.A.* **114**, 3305 (2017).

[2] S. Blinov, B. Wu, and C. Monroe, Comparison of cloud-based ion trap and superconducting quantum computer architectures (2021), [arXiv:2102.00371](https://arxiv.org/abs/2102.00371).

[3] H. J. Kimble, *Nature* **453**, 1023 (2008).

[4] S. Wehner, D. Elkouss, and R. Hanson, *Science* **362**, 303 (2018).

[5] T. J. Proctor, P. A. Knott, and J. A. Dunningham, *Phys. Rev. Lett.* **120**, 080501 (2018).

[6] X. Guo, C. R. Breum, J. Borregaard, S. Izumi, M. V. Larsen, T. Gehring, M. Christandl, J. S. Neergaard-Nielsen, and U. L. Andersen, *Nat. Phys.* **16**, 281 (2020).

[7] P. Sekatski, S. Wölk, and W. Dür, *Phys. Rev. Res.* **2**, 023052 (2020).

[8] P. Komar, E. M. Kessler, M. Bishof, L. Jiang, A. S. Sørensen, J. Ye, and M. D. Lukin, *Nat. Phys.* **10**, 582 (2014).

[9] S. Barz, E. Kashefi, A. Broadbent, J. F. Fitzsimons, A. Zeilinger, and P. Walther, *Science* **335**, 303 (2012).

[10] H. J. Briegel, W. Dür, J. I. Cirac, and P. Zoller, *Phys. Rev. Lett.* **81**, 5932 (1998).

[11] L. M. Duan, M. D. Lukin, J. I. Cirac, and P. Zoller, *Nature* **414**, 413 (2001).

[12] N. Sangouard, C. Simon, H. de Riedmatten, and N. Gisin, *Rev. Mod. Phys.* **83**, 33 (2011).

[13] K. Azuma, S. E. Economou, D. Elkouss, P. Hilaire, L. Jiang, H.-K. Lo, and I. Tzitrin, (2022), [arXiv:2212.10820](https://arxiv.org/abs/2212.10820).

[14] O. A. Collins, S. D. Jenkins, A. Kuzmich, and T. A. B. Kennedy, *Phys. Rev. Lett.* **98**, 060502 (2007).

[15] W. J. Munro, K. A. Harrison, A. M. Stephens, S. J. Devitt, and K. Nemoto, *Nature Photonics* **4**, 792 EP (2010), article.

[16] N. Sinclair, E. Saglamyurek, H. Mallahzadeh, J. A. Slater, M. George, R. Ricken, M. P. Hedges, D. Oblak, C. Simon, W. Sohler, and W. Tittel, *Phys. Rev. Lett.* **113**, 053603 (2014).

[17] P. Dhara, A. Patil, H. Krovi, and S. Guha, *Phys. Rev. A* **104**, 052612 (2021).

[18] K. Azuma, K. Tamaki, and H.-K. Lo, *Nat. Commun.* **6**, 6787 (2015).

[19] J. Borregaard, H. Pichler, T. Schröder, M. D. Lukin, P. Lodahl, and A. S. Sørensen, *Phys. Rev. X* **10**, 021071 (2020).

[20] S. Muralidharan, L. Li, J. Kim, N. Lütkenhaus, M. D. Lukin, and L. Jiang, *Sci. Rep.* **6**, 20463 (2016).

[21] S. L. N. Hermans, M. Pompili, H. K. C. Beukers, S. Baier, J. Borregaard, and R. Hanson, *Nature* **605**, 663 (2022).

[22] J. Yin, Y.-H. Li, S.-K. Liao, M. Yang, Y. Cao, L. Zhang, J.-G. Ren, W.-Q. Cai, W.-Y. Liu, S.-L. Li, *et al.*, *Nature* **582**, 501 (2020).

[23] Y. F. Pu, N. Jiang, W. Chang, H. X. Yang, C. Li, and L. M. Duan, *Nat. Commun.* **8**, 15359 (2017).

[24] J. Sperling, M. Bohmann, W. Vogel, G. Harder, B. Brecht, V. Ansari, and C. Silberhorn, *Phys. Rev. Lett.* **115**, 023601 (2015).

[25] K. Azuma, S. Bäuml, T. Coopmans, D. Elkouss, and B. Li, *AVS Quantum Science* **3**, 014101 (2021).

[26] L. Praxmeyer, (2013), [arXiv:1309.3407](https://arxiv.org/abs/1309.3407).

[27] E. Shchukin, F. Schmidt, and P. van Loock, *Phys. Rev. A* **100**, 032322 (2019).

[28] L. Kamin, E. Shchukin, F. Schmidt, and P. van Loock, *Phys. Rev. Res.* **5**, 023086 (2023).

[29] S. E. Vinay and P. Kok, *Phys. Rev. A* **99**, 042313 (2019).

[30] W. Dai and D. Towsley, (2021), [arXiv:2111.10994](https://arxiv.org/abs/2111.10994).

[31] S. Brand, T. Coopmans, and D. Elkouss, *IEEE Journal on Selected Areas in Communications* **38**, 619 (2020).

[32] B. Li, T. Coopmans, and D. Elkouss, *IEEE Transactions on Quantum Engineering* **2**, 1 (2021).

[33] T. Coopmans, S. Brand, and D. Elkouss, *Phys. Rev. A* **105**, 012608 (2022).

[34] Á. G. Iñesta, G. Vardoyan, L. Scavuzzo, and S. Wehner, *npj Quantum Information* **9**, 46 (2023).

- [35] S. Khatri, C. T. Matyas, A. U. Siddiqui, and J. P. Dowling, *Phys. Rev. Res.* **1**, 023032 (2019).
- [36] L. Bugalho, B. C. Coutinho, F. A. Monteiro, and Y. Omar, *quantum* **7**, 920 (2023).
- [37] B. V. Gnedenko, Y. K. Belyayev, and A. D. Solov'yev, *Mathematical methods of reliability theory* (Academic Press, 2014).
- [38] L. A. Gavrilov and N. S. Gavrilova, *J. Theor. Biol.* **213**, 527 (2001).
- [39] I. Bazovsky, *Reliability Theory and Practice*, Dover Civil and Mechanical Engineering Series (Dover Publications, 2004).
- [40] M. Newman, *Networks* (Oxford University Press, 2018).
- [41] R. Albert and A.-L. Barabási, *Rev. Mod. Phys.* **74**, 47 (2002).
- [42] A. Strikis, S. C. Benjamin, and B. J. Brown, Quantum computing is scalable on a planar array of qubits with fabrication defects (2021), [arXiv:2111.06432](https://arxiv.org/abs/2111.06432).
- [43] J. Rabbie, K. Chakraborty, G. Avis, and S. Wehner, *npj Quantum Inf.* **8**, 1 (2022).
- [44] E. Shchukin, F. Schmidt, and P. van Loock, *Phys. Rev. A* **100**, 032322 (2019).
- [45] W. M. Makeham, *The Assurance Magazine and Journal of the Institute of Actuaries* **8**, 301 (1860).
- [46] B. Gompertz, *Philos. Trans. R. Soc.* **115**, 513 (1825).
- [47] W. Weibull, *Gen. Litogr. Anst. Förlag* **151**, 189 (1939).
- [48] L. A. Gavrilov and N. S. Gavrilova, *The Biology of Life Span: A Quantitative Approach* (Harwood Academic, New York, 1991).
- [49] D. Steinsaltz and S. N. Evans, *Theor. Popul. Biol.* **65**, 319 (2004).
- [50] D. L. Zhou, B. Zeng, Z. Xu, and L. You, *Phys. Rev. A* **74**, 052110 (2006).
- [51] T. Kahle, E. Olbrich, J. Jost, and N. Ay, *Phys. Rev. E* **79**, 026201 (2009).
- [52] T. Galla and O. Gühne, *Phys. Rev. E* **85**, 046209 (2012).
- [53] N. Ay, J. Jost, H. Ván Lé, and L. Schwachhöfer, *Information geometry*, Vol. 64 (Springer, 2017).
- [54] F. Rozpedek, K. D. Goodenough, J. Ribeiro, N. Kalb, V. C. Vivoli, A. Reiserer, R. Hanson, S. Wehner, and D. Elkouss, *Quantum Science and Technology* (2018).
- [55] F. Rozpedek, R. Yehia, K. Goodenough, M. Ruf, P. C. Humphreys, R. Hanson, S. Wehner, and D. Elkouss, *Physical Review A* **99**, 052330 (2019).
- [56] G. Avis, R. Knegjens, A. S. Sørensen, and S. Wehner, Asymmetric node placement in fiber-based quantum networks (2023), [arXiv:2305.09635](https://arxiv.org/abs/2305.09635).
- [57] W. K. Hensinger, S. Olmschenk, D. Stick, D. Hucul, M. Yeo, M. Acton, L. Deslauriers, C. Monroe, and J. Rabchuk, *Appl. Phys. Lett.* **88**, 034101 (2006).
- [58] B. Lekitsch, S. Weidt, A. G. Fowler, K. Mølmer, S. J. Devitt, C. Wunderlich, and W. K. Hensinger, *Sci. Adv.* **3**, 1601540 (2017).
- [59] K. Hansenne, Z.-P. Xu, T. Kraft, and O. Gühne, *Nat. Commun.* **13**, 496 (2022).
- [60] G. Murta, F. Grasselli, H. Kampermann, and D. Bruß, *Adv. Quantum Technol.* **3**, 2000025 (2020).
- [61] A. Engel, *Wahrscheinlichkeitsrechnung und Statistik* (Klett, 1973).
- [62] J.-C. Walter and G. Barkema, *Physica A* **418**, 78 (2015).
- [63] Aging and reliability of quantum networks, <https://gitlab.com/alvla/aging-and-reliability-of-quantum-networks> (2023).